



HAL
open science

A computational approach to evaluate the nonlinear and noisy DC electrical response in carbon nanotube/polymer nanocomposites near the percolation threshold

Abolfazl Alizadeh Sahraei, Moosa Ayati, Denis Rodrigue, Majid Baniassadi

► To cite this version:

Abolfazl Alizadeh Sahraei, Moosa Ayati, Denis Rodrigue, Majid Baniassadi. A computational approach to evaluate the nonlinear and noisy DC electrical response in carbon nanotube/polymer nanocomposites near the percolation threshold. *Computational Materials Science*, 2020, 173, pp.109439 -. 10.1016/j.commatsci.2019.109439 . hal-03488874

HAL Id: hal-03488874

<https://hal.science/hal-03488874>

Submitted on 21 Jul 2022

HAL is a multi-disciplinary open access archive for the deposit and dissemination of scientific research documents, whether they are published or not. The documents may come from teaching and research institutions in France or abroad, or from public or private research centers.

L'archive ouverte pluridisciplinaire **HAL**, est destinée au dépôt et à la diffusion de documents scientifiques de niveau recherche, publiés ou non, émanant des établissements d'enseignement et de recherche français ou étrangers, des laboratoires publics ou privés.



Distributed under a Creative Commons Attribution - NonCommercial 4.0 International License

A computational approach to evaluate the nonlinear and noisy DC electrical response in carbon nanotube/polymer nanocomposites near the percolation threshold

Abolfazl Alizadeh Sahraei ^{a, b}, Moosa Ayati ^a, Denis Rodrigue ^b, Majid Baniassadi ^{a, c, **}

^a School of Mechanical Engineering, University of Tehran, Tehran, Iran

^b Department of Chemical Engineering, Université Laval, Quebec City G1V 0A6, Canada

^c University of Strasbourg, CNRS, ICUBE Laboratory, Strasbourg, France

Abstract

This paper presents a percolating network model to determine the electrical behavior of carbon nanotube (CNT)/polymer nanocomposites, especially near the percolation threshold. In this extended model, we considered a voltage-dependent tunneling resistance at the CNT junctions, based on Simmons' formulation. This assumption led to an electrical resistor network containing both linear and nonlinear resistance elements. We focused on extracting the continuous current-voltage (I-V) response of the nanocomposites through a recursive calculation to show the ability of the model to simulate the nonlinear and noisy behavior of the I-V curve in CNT/polymer systems. The effects of CNT diameter, length, concentration, and intrinsic conductance, as well as the tunneling gap at the junctions and matrix dielectric constant, were also investigated and discussed. Our results revealed that the nonlinearity in I-V curves near the percolation threshold is related to the voltage-dependent nature of the tunneling resistance. The number of junctions and equivalent CNT length in the percolation pathway are two effective parameters controlling the electrical behavior of CNT/polymer nanocomposites. The results obtained are also in good agreement with our previous experimental data on CNT/epoxy nanocomposite and confirmed

** Corresponding author. Tel: +98 918 162-1480. E-mail: m.baniassadi@ut.ac.ir (Majid Baniassadi).

that the proposed model can efficiently predict the I-V characteristic curves for CNT/polymer composites.

Keywords:

DC electrical response; I-V curve; Nonlinearity; Noisy behavior; CNT/Polymer composites; Percolation network model

1. Introduction

Scientific and commercial interests for electrically conductive polymer nanocomposites have rapidly grown in the past decade [1-3]. This popularity originates from their lightweight, low cost, ease of processing, acceptable corrosion resistance, as well as unique mechanical and electrical properties. Thin polymer nanocomposite films, especially those reinforced by carbon nanotubes (CNT), have brought interesting opportunities to produce multifunctional materials [4, 5]. In particular, the development of CNT/polymer nanocomposites led to a wide range of applications, including electromagnetic interference shielding, highly sensitive strain sensors, photovoltaic cells, etc. [3, 6].

Several investigations took advantage of numerical simulations to predict the bulk electrical properties and better understand the underlying mechanism of electrical conduction in CNT/polymer composites [7-12]. In general, three types of resistances are defined in such systems: 1) the intrinsic resistance of conducting fillers, 2) the direct contact resistance between fillers, and 3) the tunneling resistance of adjacent fillers [8]. Previous results have shown that the tunneling resistance plays a dominant role in the electrical properties of CNT-based composites, especially around the percolation threshold [7, 13, 14]. For instance, Ounaies et al. [15] reported

a nonlinear behavior of the current-voltage (I-V) curve for single-walled carbon nanotube (SWCNT)/polyimide composites. They suggested that this behavior is a clear indication of quantum tunneling conduction. Hu et al. [16] also reported the same I-V trends for a 0.35 wt.% SWCNT/polydimethylsiloxane composite, while this nonlinearity vanished for the sample at 5 wt.% SWNCT. Recently, Alizadeh Sahraei et al. [17] extracted I-V curves for different CNT weight fractions in epoxy nanocomposites and reported their respective equivalent circuits. The results revealed that the characteristic I-V curve of 0.2 wt.% CNT/epoxy was nonlinear, while the curves were linear for higher CNT content.

Despite the importance of the tunneling phenomena in the electrical properties of CNT/polymer composites, the majority of published papers did not include the tunneling effect in their numerical simulations, but they still found good agreement with experimental results. Our observations revealed two main reasons for this agreement. Firstly, most of these investigations modeled the electrical properties of composites far from the percolation threshold. Higher deviations from experimental results have been observed for the samples near percolation. The second reason is that most of these investigations reported equivalent electrical conductivity (or resistance) of CNT/polymer composites in a single point, and no characteristic I-V curves had been reported/modeled in their simulations. For example, Hu et al. [18] investigated the electrical behavior of CNT/polymer nanocomposites close to and above the percolation threshold, without considering the tunneling effect and contact resistance. The effect of CNT aspect ratio and curvature was nevertheless included. Lee and Loh [19] implemented a 2D percolation-based model to investigate the piezoresistivity of CNT/polymer nanocomposites. They applied constant values as the Ohmic and junction resistances, but again the tunneling effect was not considered in the simulation. They modeled the piezoresistive response far above percolation and validated

their numerical results with experiments. They also followed a similar modeling approach in other investigations [9, 20].

Taking into account the contact and tunneling resistances adds some complexities to numerical modeling, but more accurate simulation results are expected [7, 8, 11, 14, 21, 22]. Hu et al. [21] modeled the piezoresistivity of CNT/epoxy composite by considering the effect of tunneling resistance. The results showed a nonlinear piezoresistive response at low CNT loading and at strains higher than 0.2%, an indication that the tunneling effect was prevailing under these conditions. Rahman and Servati [22] proposed a numerical model to investigate the effect of inter-tube tunneling and other CNT physical properties such as concentration and type of polymer matrix. The numerical results showed that higher composite conductivity is obtained by considering the tunneling effect, especially close to percolation. By using Simmons' formula to model the tunneling resistance [23, 24], Li et al. [7] predicted the conductivity of CNT/epoxy nanocomposites as a function of contact resistance. From their simulation results, it was concluded that the critical tunneling distance (*CTD*) in CNT/polymer composites is 1.8 nm. They also reported that contact resistance plays a dominant role in the electrical properties of such composites. Using the Landauer-Buttiker (L-B) formula, Bao et al. [8] proposed a model to predict the electrical conductivity of CNT/polymer nanocomposites. They showed that the direct contact resistance between every pair of crossing CNT is the result of electron ballistic tunneling between them. Based on the L-B formula, the minimum direct contact resistance is equal to the value of the tunneling resistance occurring at the smallest CNT separation, which is the van der Waals separation distance.

Despite all these investigations, there are still some open questions concerning the effect of each parameter on the macroscopic properties of CNT based nanocomposites. For example, can the

existing models capture the nonlinear and noisy behavior of the I-V characteristic curve in CNT/polymer nanocomposite? What is the main reason for this nonlinearity in the I-V curves near the percolation threshold? How does accounting for the tunneling resistance leads to nonlinear behavior of the I-V curve and better prediction of the electrical properties near percolation? Based on Simmons' formula [23], the tunneling resistance is a function of the voltage across the thin insulating film between two electrodes. However, to the best of the authors' knowledge, there is no investigation including the voltage dependency of the tunneling resistance to predict the I-V characteristics curve of CNT/polymer composites. Here, a new recursive procedure is introduced to model the I-V characteristic curves and electrical properties of CNT/polymer nanocomposites by a combination of the statistical Monte Carlo method, Simmons' formula, and modified nodal analysis. The obtained numerical results were also compared with the I-V curves of our previous work on multiwalled carbon nanotube (MWCNT)/epoxy composites [17]. We believe that our simulation procedure and results provide a deeper understanding of the tunneling resistance and electrical properties in CNT/polymer nanocomposites.

2. Modeling and Simulation Procedure

As an effort to elucidate the electrical properties and especially the nonlinear behavior of the I-V curves of CNT/polymer films, a modified 2D soft-core percolation-based model was used. Based on the literature, the soft-core model seems to contradict the fact that CNT cannot penetrate each other. So, it is assumed here that the CNT can overlap at contact points [7, 14, 25]. This assumption not only substantially decreases the computational cost, but can also produce a very reliable prediction for electrical properties.

To build a 2D resistor network model (Fig. 1a), each CNT is assumed to be straight and randomly distributed in a 2D square representative volume element (RVE). The RVE area was fixed at $100 \times 100 \mu\text{m}^2$. As shown in Fig. 1a, each CNT was defined by a line segment. The first end-point of the i^{th} CNT, $P_{1i} = (x_{1i}, y_{1i})$, was described by:

$$\begin{aligned} x_{1i} &= L_{box} * rand, \\ y_{1i} &= L_{box} * rand, \end{aligned} \tag{1}$$

where L_{box} is the RVE size in the x - and y -directions, while $rand$ is a uniformly distributed random number in the $[0, 1]$ interval (the $rand$ function in MATLAB). The end-point of the i^{th} CNT, $P_{2i} = (x_{2i}, y_{2i})$, was identified as:

$$\begin{aligned} x_{2i} &= x_{1i} + L_{CNT} \cos \theta, \\ y_{2i} &= y_{1i} + L_{CNT} \sin \theta. \end{aligned} \tag{2}$$

Here, L_{CNT} represents the CNT length, and θ denotes a randomly generated CNT orientation in the $[0, 2\pi]$ domain. This procedure was performed for CNT addition until the prescribed number of CNT was inserted into the RVE. To ensure the existence of a predetermined number of CNT in the RVE, the fragments of CNTs that were outside the boundaries were cut and then moved back into RVE through the opposite face [14, 26].

After generating the CNTs, the shortest distance between each pair of CNT was calculated to find the percolation path in the x -direction. In this study, we considered the tunneling effect between adjacent CNTs. Therefore, two types of intersections were defined: direct physical contact when the distance between CNT pairs is zero or less than “ D ” and tunneling contact when the distance is less than “ $D + CTD$,” where D is the CNT diameter, and CTD is the critical tunneling distance [7, 8]. Since the CNTs are straight, junction locations are simply identified by solving sets of linear equations corresponding to each CNT pairs. All the junction locations are

numbered and stored in a junction matrix. After reaching percolation, the CNTs not included in a percolation cluster are neglected, because they do not contribute to the current flow as the main conduction path is through the percolation network.

Three types of resistances are present in the system: the intrinsic CNT resistance, contact resistance, and tunneling resistance (Fig. 1b). The intrinsic CNT resistance is defined along one CNT between two nearest junctions (R_{CNT} in Fig. 1b) and can be evaluated as [8]:

$$R_{CNT} = \frac{4l_{CNT}}{g_{CNT}\pi D^2} \quad (3)$$

where l_{CNT} is the CNT length between two nearest nodes in the neighboring CNT, and g_{CNT} is the homogenized intrinsic CNT electrical conductivity.

The contact and tunneling resistances are evaluated by Simmons's formula [23, 27]. Based on the generalized Simmons's equations for similar electrodes [23], the tunneling resistance depends on different factors such as the insulating layer thickness and type of material, the electrodes work function, the voltage between electrodes, etc. Here, before applying Simmons's formula, a modification on the direct contact nodes is made. Based on the Pauli exclusion principle, the equilibrium distance between two carbon atomic structures cannot be less than the van der Waals separation distance (d_{vdw}), which is around 0.34 nm [26, 28, 29]. On the other hand, the diameter of different polymer molecules is greater than 0.4 nm, which is the diameter of polyethylene oligomers [30, 31]. Therefore, if two CNT are in direct contact, we manually separate them to avoid penetration ($d_{separation}$), then replace the junction node with two detached nodes, and finally add a contact resistance ($R_{contact}$) between them (Fig. 1c). Additionally, if the closest distance between two CNT is in the $[D + d_{separation}, D + CTD]$ range, a tunneling resistance ($R_{tunneling}$) between them is added (Fig. 1d). The junction matrix and number of junctions are updated in this step.

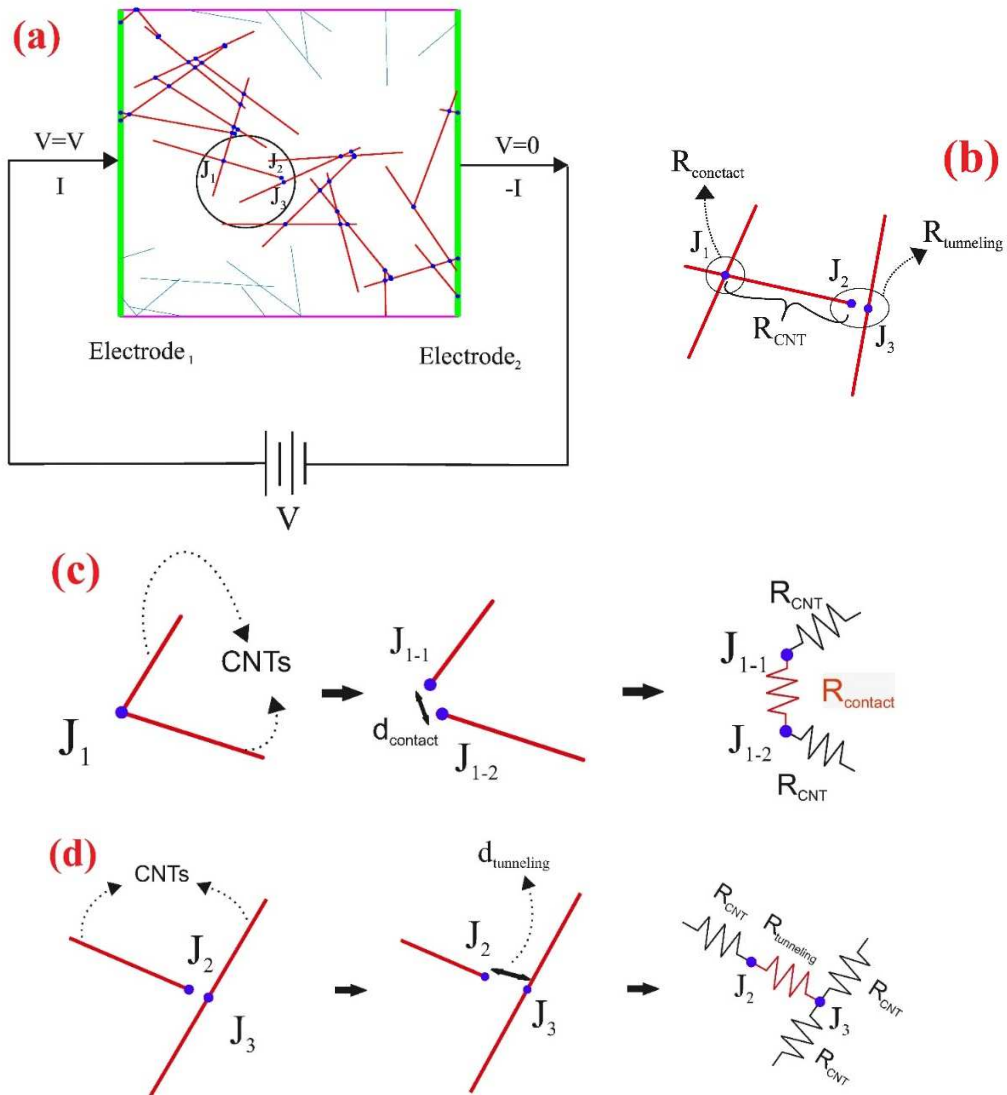


Fig. 1: Schematic representation of: a) the resistor model with a random CNT distribution (red lines are CNTs in the percolation cluster), b) three different types of resistances in the percolating network, c) modification on direct contact nodes, and d) a CNT pair with a tunneling gap and resistance.

Assuming uniform thickness for the insulating film in the contact area and neglecting the variation of barrier height along the thickness (i.e., the distance between two electrodes (CNT here) is homogeneously filled by the polymer matrix), a rectangular barrier with imaged force was included to determine the contact and tunneling resistances [23]. Based on the applied voltage across the thin film (U), two cases can be studied.

For $U \approx 0$ [23]:

$$J = 3.6 * \frac{10^{10}}{\Delta s} \sqrt{\varphi_L} U e^{-1.025\Delta s\sqrt{\varphi_L}} \quad (4)$$

where

$$\varphi_L = \varphi_0 - \frac{5.75}{K\Delta s} - \ln \frac{s_2(s - s_1)}{s_1(s - s_2)} \quad (5)$$

and

$$s_1 = \frac{6}{K\varphi_0} \quad (6)$$

$$s_2 = s - \frac{6}{K\varphi_0}$$

where J is the current density penetrating through the insulating film (A/cm^2), $\Delta s (= s_2 - s_1)$ is the difference of limits of the barrier at Fermi level, φ_0 is the height of the rectangular barrier (V), K is the dielectric constant of the insulating film material, and s is the thickness of the insulating layer (\AA).

For other U values [23]:

$$J = 6.2 * \frac{10^{10}}{\Delta s^2} \{ \varphi_I e^{-1.025\Delta s\sqrt{\varphi_I}} - (\varphi_I + U) e^{-1.025\Delta s\sqrt{(\varphi_I + U)}} \}, \quad (7)$$

where

$$\varphi_I = \varphi_0 - \frac{U}{2s}(s_1 + s_2) - \frac{5.75}{K\Delta s} \ln \frac{s_2(s - s_1)}{s_1(s - s_2)} \quad (8)$$

For $U < \varphi_0$:

$$s_1 = \frac{6}{K\varphi_0} \quad (9)$$

$$s_2 = s \frac{1 - 46}{3\varphi_0 K s + 20 - 2U K s} + \frac{6}{K\varphi_0}$$

For $U > \varphi_0$:

$$s_1 = \frac{6}{K\varphi_0}$$

$$s_2 = \frac{\varphi_0 Ks - 28}{KU}$$
(10)

The tunneling resistance is then evaluated by:

$$R_{tunneling} = \frac{U}{JA_c}$$
(11)

where A_c is the contact area at the overlapping position. For simplicity, by neglecting the relative orientation between each pair of CNT, A_c is approximated by $A_c = D^2$. It is important to note that both contact and tunneling resistances are calculated by Eq. (4-11), with the difference that for contact resistance, the thickness of the insulating layer (s) is assumed to be constant (equal to $d_{separation}$), while for the tunneling resistance, s can take different values in the $[D + d_{separation}, D + CTD]$ range.

From Simmons's formula (Eq. 4-11), the tunneling resistance is a function of the voltage across the insulating layer. Therefore, it is essential to obtain the voltages for all junction nodes in the system. To do so, a modified nodal analysis is applied to the network resistance with an independent voltage source (Fig. 1a) [9, 19, 32]. The voltage of all nodes and current through the voltage source was obtained using Kirchhoff's current law and the conductance version of Ohm's law as:

$$[G]\{v\} = \{I\}$$
(12)

where $[G]$ is the conductance matrix, $\{I\}$ is the equivalent current vector, and $\{v\}$ is the unknown nodal voltage vector. $[G]$ is a symmetric square matrix of order n , where n is the total number of junctions minus the reference node. The positive diagonal components, G_{kk} , is the sum of the conductance values directly connected to node k , while the negative off-diagonal components,

G_{kj} , is the negative of the equivalent conductance directly connecting node k to node j . It is assumed that electrode₁ and electrode₂ are the source and drain electrodes with potential V and 0 , respectively (Fig. 1a).

Then, a recursive calculation to find the current values across the voltage source is performed. Potential differences between 0 and 6 V, with 0.1 V steps, are applied across the electrodes to excite the system. To build the conductance matrix, the values of all resistances in the resistor network for each voltage must be known. Since the nodal voltages in the first step are not available before solving Eq. (12), a constant voltage (U) across all tunneling resistances is assumed. With this initial guess, the nodal voltages (v_i) and the equivalent current matrix $\{I\}$ of the network are evaluated. In the next step, the contact and tunneling resistances are calculated based on the obtained nodal voltages (v_i), and Eq. (12) is solved again to obtain the updated nodal voltages (v_{i+1}) and equivalent current. This iterative procedure is repeated until a stopping criterion is reached. The stopping criterion is based on the following error function:

$$error = \sum (\{v_{i+1}\} - \{v_i\})^2 \quad (13)$$

where v_{i+1} and v_i are the vectors of nodal voltages at two successive steps. At each voltage, the calculation continues until the stop criterion is met (error of 10^{-20} here). A flowchart of the computational procedure is illustrated in Fig. 2.

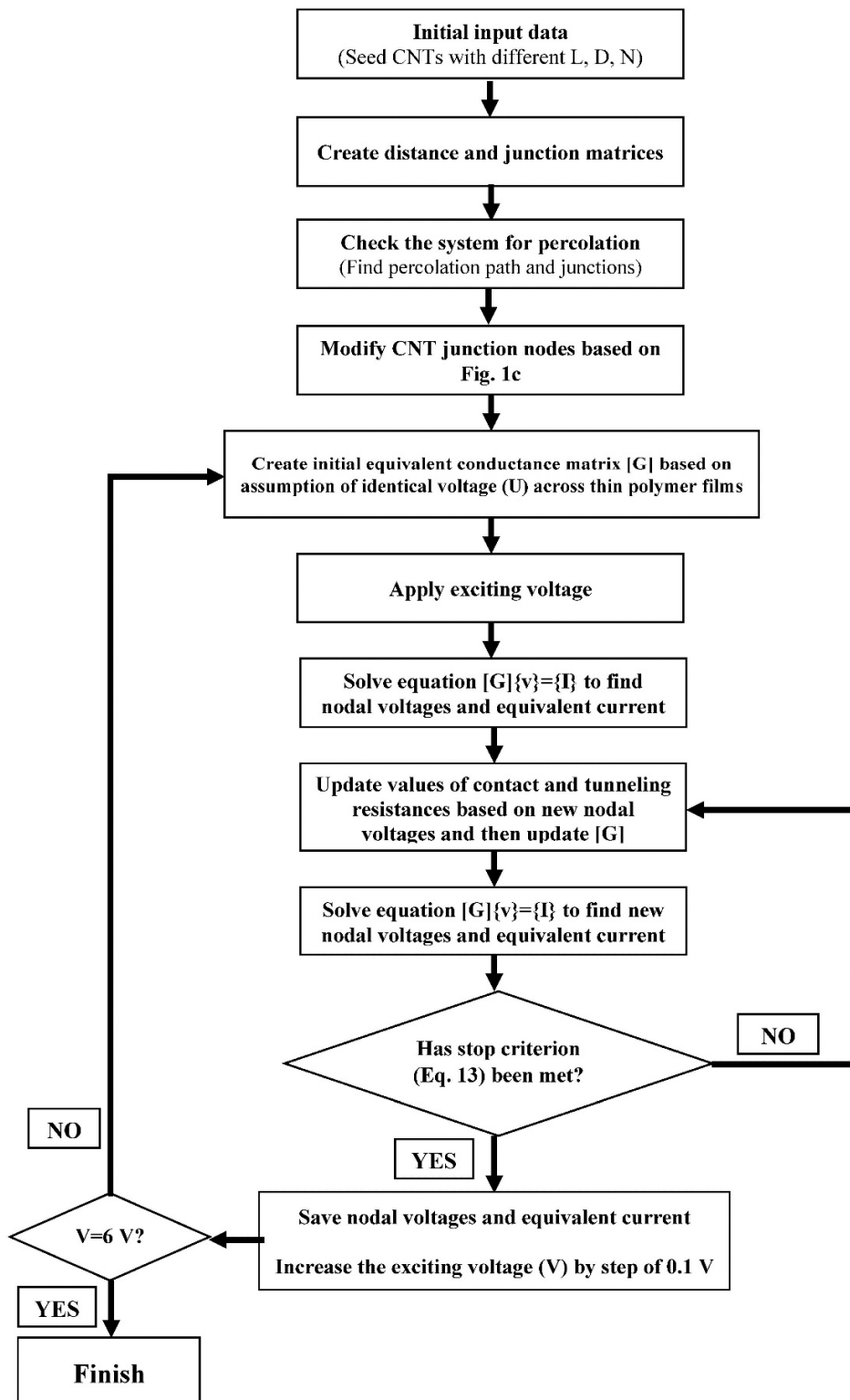


Fig. 2: The computational procedure suggested for extracting the I-V curve.

3. Results and Discussion

3.1 Numerical evaluation of tunneling resistivity

Fig. 3 presents the tunneling resistance as a function of the voltage across a junction using Eq. (4-11). Whenever needed, the dielectric constant of epoxy ($K = 3.98$) and the work function of CNT ($\phi_0 = 5$ eV) were used in the calculations [33]. Also, the CNT diameter and tunneling distance were taken as 50 nm and 1 nm, respectively.

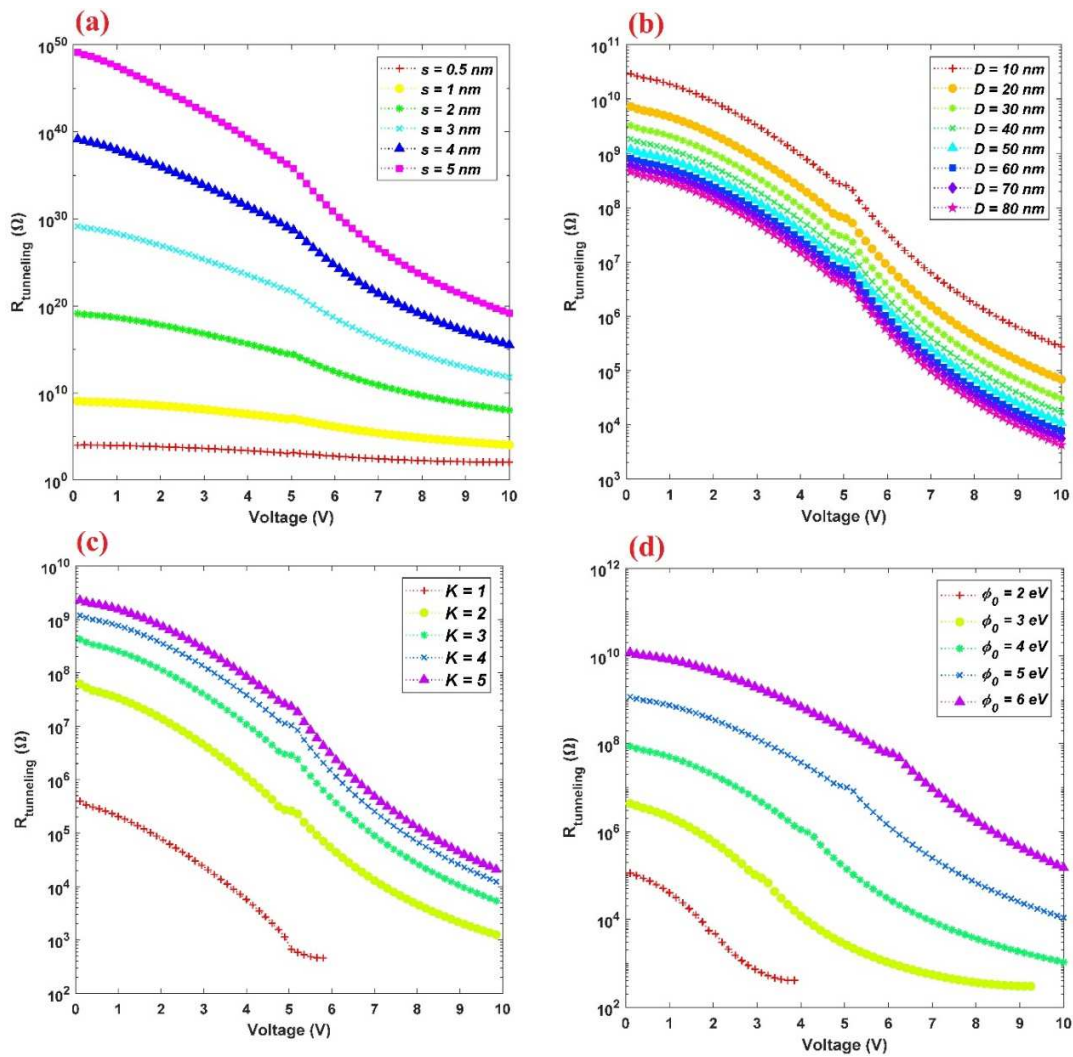


Fig. 3: Theoretical $R_{\text{tunneling}}$ -Voltage characteristic curves of tunnel junctions as a function of: a) tunneling distance (s), b) CNT diameter (D), c) dielectric constant of the insulating polymer (K), and d) height of rectangular barrier (ϕ_0) using the following parameters as a base of comparison: $D = 50$ nm, $s = 1$ nm, $K = 3.98$, and $\phi_0 = 5$ eV.

As seen in Fig. 3a, increasing the insulating film thickness substantially increases the tunneling resistance. In fact, for the given values of D and φ_0 , the electrons cannot flow through the insulating layer when the tunneling distance is greater than 2 nm. Therefore, the critical tunneling distance was assumed to be 2 nm for the electric tunneling effect in the calculations. The tunneling resistance varies moderately with increasing CNT diameter (Fig. 3b). For instance, the tunneling resistance at low voltages decreases by only two orders of magnitude (from 10^{10} to $10^8 \Omega$) by increasing the CNT diameter from 10 to 80 nm. The insulating material is another important parameter affecting the tunneling resistance (Fig. 3c) so that increasing the dielectric constant (K) leads to higher tunneling resistance values. The difference between the $R_{\text{tunneling}}$ -Voltage curves becomes less with increasing K . The work function of the electrodes also has a significant effect on the tunneling resistance of a junction (Fig. 3d). Based on Eq. (3) and Fig. 3d, it can be concluded that different fillers play at least two roles in the equivalent resistance of such composites: one by their intrinsic resistances and the other by influencing contact resistance or more generally the tunneling resistance.

3.2 Effect of different parameters on the electrical behavior of CNT/polymer nanocomposites

In the current 2D model, the percolation probability test was performed to understand the percolation behavior of the CNT/polymer nanocomposites [34]. The percolation probability (P) can be calculated as:

$$P = \frac{n_p}{n_t} \quad (14)$$

where n_t is the total number of simulations, and n_p is the number of simulations in which the model showed at least one conductive path in the x -direction. To extract the percolation probability graph, 100 simulations were conducted for each CNT density (i.e., number of CNT or N) at different lengths. Fig. 4 presents the percolation probability plot as a function of CNT

length. The CNT diameter was assumed to be 50 nm in all samples.

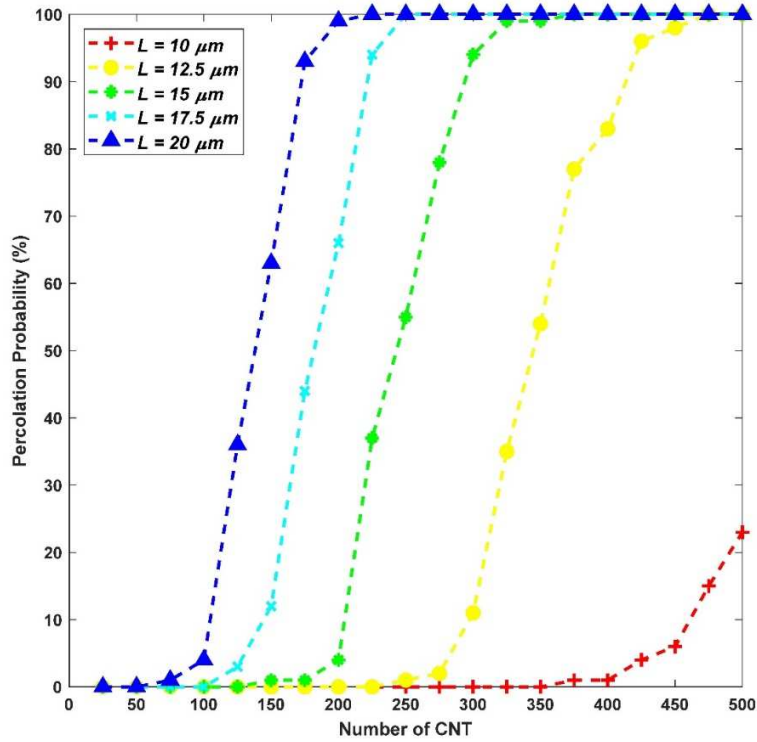


Fig. 4: Percolation probability of CNT-based nanocomposites as a function of CNT length. The RVE size and CNT diameter were assumed to be $100 \times 100 \mu\text{m}^2$ and 50 nm, respectively.

These results give valuable insight into regions close to and far from percolation. Based on the definition, the percolation threshold is obtained as the CNT density giving a 50% probability [19, 34]. As expected, fewer CNT was required for longer nanotubes to percolate the system. Defining an equivalent filler length as the product between the CNT number and length ($N \times L_{CNT}$), which serves as an indirect representation of the volume fraction, it can be concluded that longer CNTs percolate at lower volume fractions. When the percolation probability is 100%, this means that the system is percolated for any random configurations. For example, the number of CNT corresponding to a 100% percolation probability increases from 200 to 450 by decreasing the CNT length from $20 \mu\text{m}$ to $12.5 \mu\text{m}$.

Fig. 5 presents the effect of CNT length and concentration on the bulk electrical resistance of CNT/polymer nanocomposites. In this part, three CNT lengths ($L_{CNT} = 15, 17.5, \text{ and } 20 \mu\text{m}$) were used because smaller CNTs have a very limited probability of creating a percolation path when $N = 225$ or less.

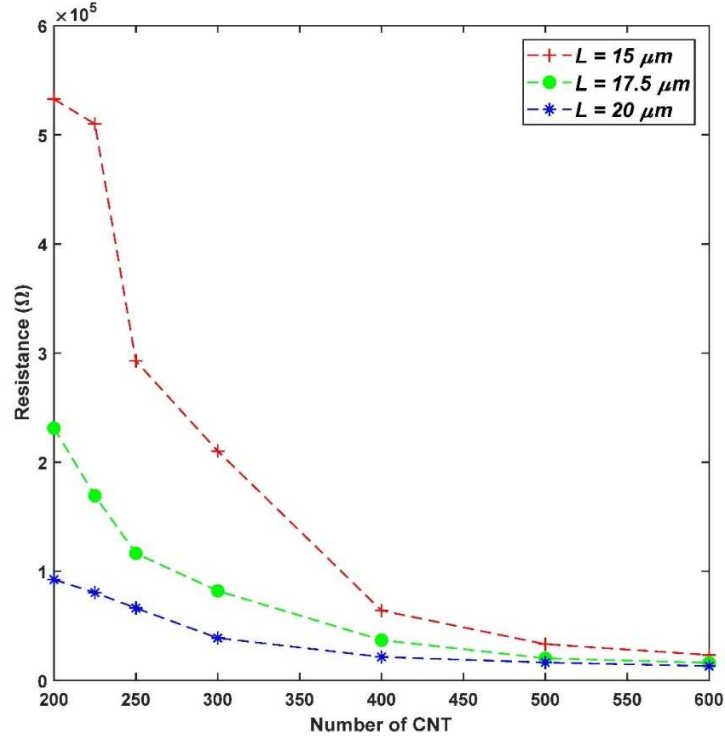


Fig. 5: Variation of the electrical resistivity of the bulk nanocomposites as a function of CNT length and concentration at $V = 3 \text{ V}$. The following parameters were used for the simulations: RVE size = $100 \times 100 \mu\text{m}^2$, $D = 50 \text{ nm}$, $d_{\text{separation}} = 0.47 \text{ nm}$, $g_{CNT} = 10^5 \text{ S/m}$, $K = 3.98$ and $\varphi_0 = 5 \text{ eV}$.

Based on the results of Hu et al. [26] for the CNT/epoxy system, the separation distance at junctions ($d_{\text{separation}}$) was chosen to be 0.47 nm . The experimental results revealed that the intrinsic MWCNT conductivity (g_{CNT}) ranges from 5×10^3 to $5 \times 10^6 \text{ S/m}$ [35, 36]. So, an intermediate value was selected: $g_{CNT} = 1 \times 10^5 \text{ S/m}$. Since the stimulated voltage is also important to calculate the contact and tunneling resistances, a voltage of 3 V was used to extract the electrical resistance values. The other parameters were chosen as: $D = 50 \text{ nm}$, $CTD = 2 \text{ nm}$,

$K = 3.98$ and $\varphi_0 = 5$ eV. The average value of 50 simulations for each case is reported in Fig. 5. It can be seen that increasing the CNT concentration leads to a plateau for the composite resistance because the number of electrical paths is saturated at higher CNT concentration. Moreover, the longer the CNT (or the aspect ratio), the lower is the nanocomposites electrical resistivity. This behavior stems from the fact that longer CNTs create more intersections with each other, leading to a higher number of conductive pathways and lower electrical resistivity. Again, the difference between the bulk resistance values becomes smaller with increasing CNT concentrations.

Fig. 6 summarizes the contribution of the different parameters on the I-V curves of the CNT based nanocomposites. For reliable comparisons, the parameter study was applied on a random constant structure with $N = 150$ nanotubes of $20 \mu\text{m}$ in length inside a square RVE of $100 \times 100 \mu\text{m}^2$. Whenever needed, the following parameters were used in the calculations: $D = 50$ nm, $K = 3.98$, $\varphi_0 = 5$ eV, $d_{\text{separation}} = 0.47$ nm and $g_{\text{CNT}} = 10^5$ S/m.

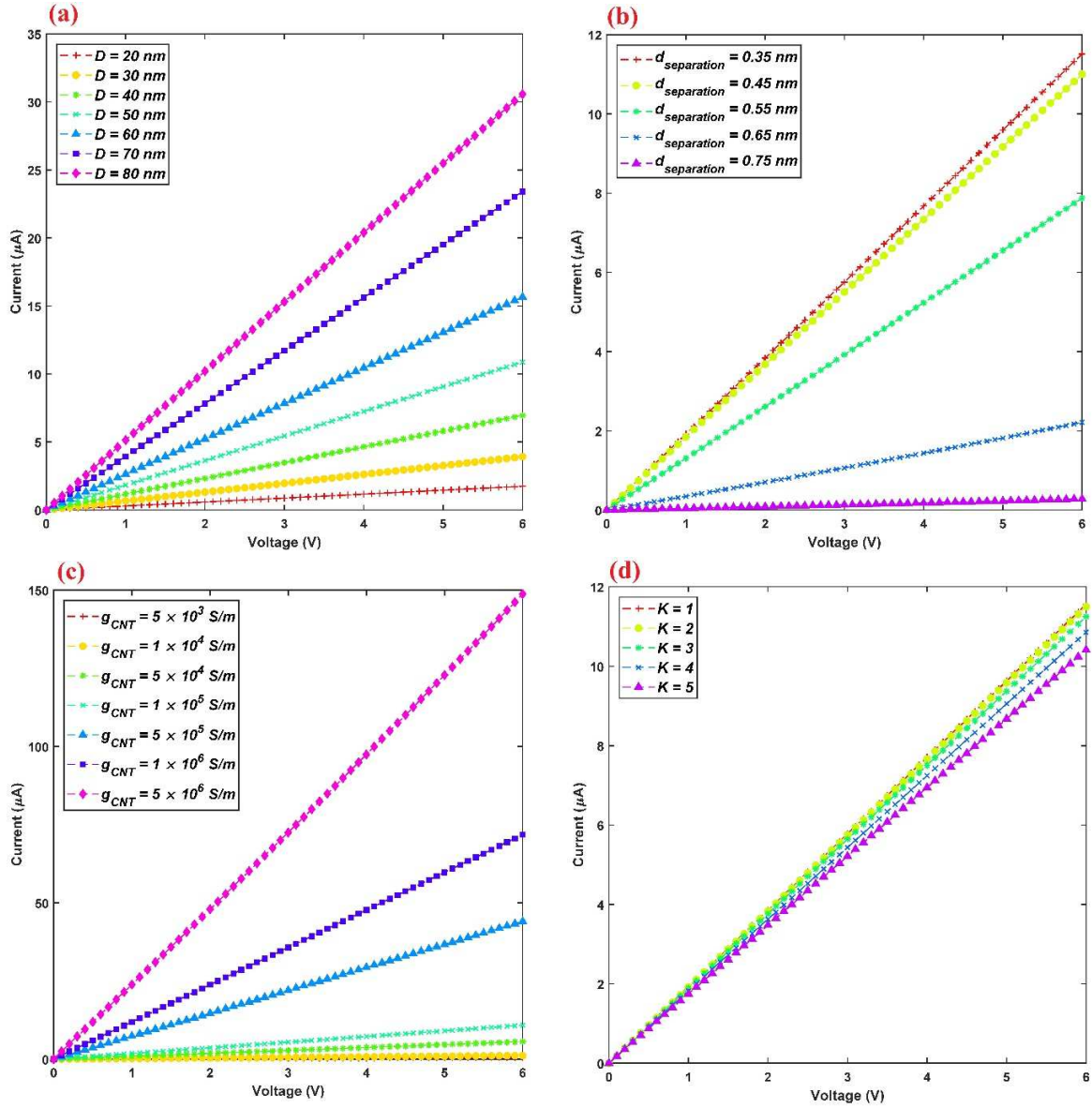


Fig. 6: Comparison of I-V curves for a composite with $N = 150$ nanotubes with different: a) CNT diameter (D), b) thickness of the insulating film at junctions ($d_{\text{separation}}$), c) intrinsic electrical conductivity of CNT (g_{CNT}), and d) dielectric constant of the matrix material (K). For the calculations, $L_{\text{CNT}} = 20 \mu\text{m}$, $D = 50 \text{ nm}$, $d_{\text{separation}} = 0.47 \text{ nm}$, $g_{\text{CNT}} = 10^5 \text{ S/m}$, $K = 3.98$ and $\varphi_0 = 5 \text{ eV}$ when needed. The RVE size was $100 \times 100 \mu\text{m}^2$.

As seen in Fig. 6a, incorporation of CNT with larger diameter leads to higher conductivity of the CNT/polymer composites. This is expected since increasing the CNT diameter leads to two favorable effects: decreasing the CNT intrinsic resistance (Eq. 3), and decreasing the tunneling

resistance (Fig. 3b). CNT with a larger diameter is more conductive and also show lower $R_{tunneling}$ at the direct and tunneling junctions. The electrical resistance of CNT based composites strongly depends on the contact resistance of intersected CNT (Fig. 6b). Increasing the insulating layer thickness from 0.35 to 0.75 nm substantially increases $R_{tunneling}$ by four orders of magnitude at low voltages (Eq. 4-11). As seen in Fig. 6b, the slope of the I-V curves is lower with increasing $d_{separation}$, showing the opposite relationship between $d_{separation}$ and bulk conductivity. For instance, at a voltage of 6 V, increasing $d_{separation}$ from 0.35 to 0.75 nm increases the composite bulk resistance from 5.2×10^5 to $2.2 \times 10^7 \Omega$.

The effect of g_{CNT} (or R_{CNT}) on the I-V curves is shown in Fig. 6c. When g_{CNT} is in the order of 10^3 to 10^4 S/m, then the bulk conductivity shows a weak dependence on the R_{CNT} value, while for higher g_{CNT} values, the composite conductivity substantially increases by decreasing R_{CNT} . The matrix material (i.e., K) also has a small effect on the I-V curves of CNT/polymer nanocomposites, as shown in Fig. 6d. The contribution of the matrix material to the electrical behavior arises from the tunneling effect in this model. If the tunneling effect is not accounted for, then the composite conductivity would only depend on the CNT distribution quality and intrinsic properties. However, the use of different polymers as the matrix changes the bulk electrical behavior of CNT/polymer nanocomposites. The results of Fig. 6d confirm the effect of the matrix materials on the electrical behavior of CNT/polymer nanocomposites.

To elucidate the effect of the CNT length on the I-V characteristic curves, a series of simulations on the CNT/epoxy nanocomposites were performed on different composite configurations with different CNT lengths, but the equivalent CNT length (i.e., the relative volume fraction) was maintained constant in all the samples. An equivalent CNT length of 5000 μm was fixed resulting into $N = 500, 400, 333, 286,$ and 250 nanotubes for $L_{CNT} = 10, 12.5, 15, 17.5$ and 20

μm , respectively. The simulation results in Fig. 7 show that the incorporation of longer CNT at constant volume fraction leads to improved electrical conductivity. A clear difference between the I-V curves of the composites with $L_{CNT} = 10 \mu\text{m}$ and other samples is also observed in Fig. 7. The difference can be roughly explained by the results of the percolation probability (Fig. 4). The results in Fig. 4 show that for $N = 500$ and $L_{CNT} = 10 \mu\text{m}$, the sample is close to the percolation region, while the other samples are far above the percolation threshold. Therefore, due to a larger number of conductive pathways, better electrical conductivity is observed for samples far above the percolation threshold.

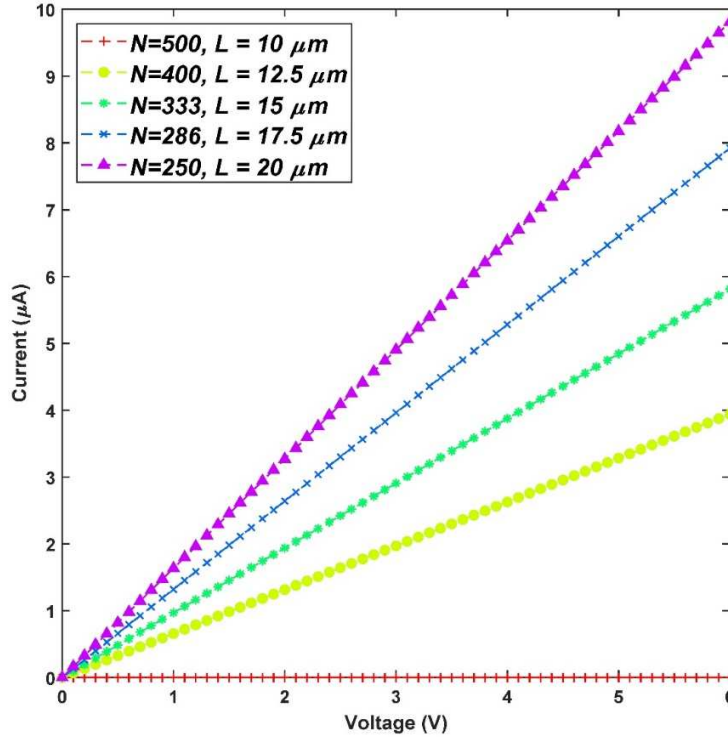


Fig. 7: Effect of CNT length on the characteristic I-V curves for nanocomposites at a constant equivalent filler length of $5000 \mu\text{m}$. The RVE size is $100 \times 100 \mu\text{m}^2$. The following parameters were used: $D = 50 \text{ nm}$, $d_{\text{separation}} = 0.47 \text{ nm}$, $g_{CNT} = 10^5 \text{ S/m}$, $K = 3.98$ and $\varphi_0 = 5 \text{ eV}$.

To further investigate the reasons for the linear and nonlinear behavior of I-V curves, some characteristic parameters for the nanocomposites in Fig. 7 are summarized in Table 1.

Table 1: Results for the composites presented in Fig. 7. Note that $N_{\text{percolation}}$ is the number of CNT in the percolation cluster, N_{total} is the total number of CNT in the composite, $L_{\text{CNT_Percolation}}$ is the equivalent CNT length in the conduction path, $L_{\text{CNT_total}}$ is the total equivalent CNT length in the composite (5000 μm for all composites), and $N_{\text{junctions}}$ is the number of CNT junctions in the composite.

Sample	N = 500 $L_{\text{CNT}} = 10 \mu\text{m}$	N = 400 $L_{\text{CNT}} = 12.5 \mu\text{m}$	N = 333 $L_{\text{CNT}} = 15 \mu\text{m}$	N = 286 $L_{\text{CNT}} = 17.5 \mu\text{m}$	N = 250 $L_{\text{CNT}} = 20 \mu\text{m}$
$\frac{N_{\text{percolation}}}{N_{\text{total}}}$	0.37	0.65	0.84	0.88	0.91
Number of R_{CNT}	207	324	448	439	466
Number of junctions (R_{contact})	429	624	815	798	811
Equivalent CNT length in the conduction path (μm)	1147	2123	3002	3288	3457
$\frac{L_{\text{CNT_percolation}}}{L_{\text{CNT_total}}}$	0.23	0.42	0.60	0.66	0.69
$\frac{L_{\text{CNT_percolation}}}{N_{\text{junctions}}}$	2.67	3.40	3.68	4.12	4.26

$\frac{N_{\text{percolation}}}{N_{\text{total}}}$ represents the CNT contribution in the percolation cluster. As can be seen, its value increases from 37% to 91% with increasing CNT length. At the same time the equivalent CNT length in the percolated cluster increases by three times by increasing the CNT length from 10 to 20 μm . The $\frac{L_{\text{CNT_percolation}}}{L_{\text{CNT_total}}}$ ratio is obtained by dividing the equivalent CNT length in the percolation cluster by the total equivalent CNT length (5000 μm in the current calculations). In this study, a criterion, namely $\frac{L_{\text{CNT_percolation}}}{N_{\text{junctions}}}$, is introduced to better analyze the results. The

$\frac{L_{\text{CNT_percolation}}}{N_{\text{junctions}}}$ ratio indicates the average R_{CNT} length per junction. With increasing the $\frac{L_{\text{CNT_percolation}}}{N_{\text{junctions}}}$ ratio, the dominant conduction mechanism changes from tunneling conductance to intrinsic filler conductance. In other words, increasing the CNT length (and

subsequently the $\frac{L_{CNT_{percolation}}}{N_{junctions}}$ ratio) leads to the domination of linear resistance elements (R_{CNT}) over nonlinear resistance elements ($R_{contacts}$), which itself determines the overall behavior of I-V curves in CNT/polymer nanocomposites.

To better understand the electrical behavior and conduction mechanism in CNT/polymer nanocomposites, the microstructures and the respective I-V curves of two nanocomposites with different numbers of nanotubes ($N = 500$ and 650) of $10 \mu\text{m}$ length are presented in Fig. 8. The nonlinear relation between the voltage and the current is clearly seen in Fig. 8b for the sample with 500 nanotubes. As mentioned before, this nanocomposite is close to percolation with $N = 500$ nanotubes of $L_{CNT} = 10 \mu\text{m}$. In this case, the CNT distribution in the RVE (Fig. 8a) shows that less than half of the CNT is in the percolation path, while for the sample with 650 nanotubes of the same length, almost all of the CNT contributed in electron conduction (Fig. 8c). In the latter case, there is a linear relationship between current and voltage, as shown in Fig. 8d. It is important to note that after reaching percolation, two mechanisms still contribute to the nanocomposite electrical conduction: one is the conduction through CNTs, and the other is the conduction through tunneling junctions. Thus, the equivalent resistance network in CNT/polymer nanocomposites contains two types of resistance: 1) linear (R_{CNT}), and 2) nonlinear ($R_{contact}$ and $R_{tunneling}$). The nonlinear resistances are a function of potential differences between two junction end nodes, as described by Simmons' formula. Therefore, a variation of the stimulating voltage modifies the junction resistances values, and thus the equivalent resistance network between two source and drain electrodes. The nonlinear behavior of the I-V curve originates from the dominant role of the nonlinear tunneling resistances at junctions near the percolation state. In fact, the voltage-dependent nature of the tunneling resistance is the main reason for the observed nonlinear I-V curve near percolation.

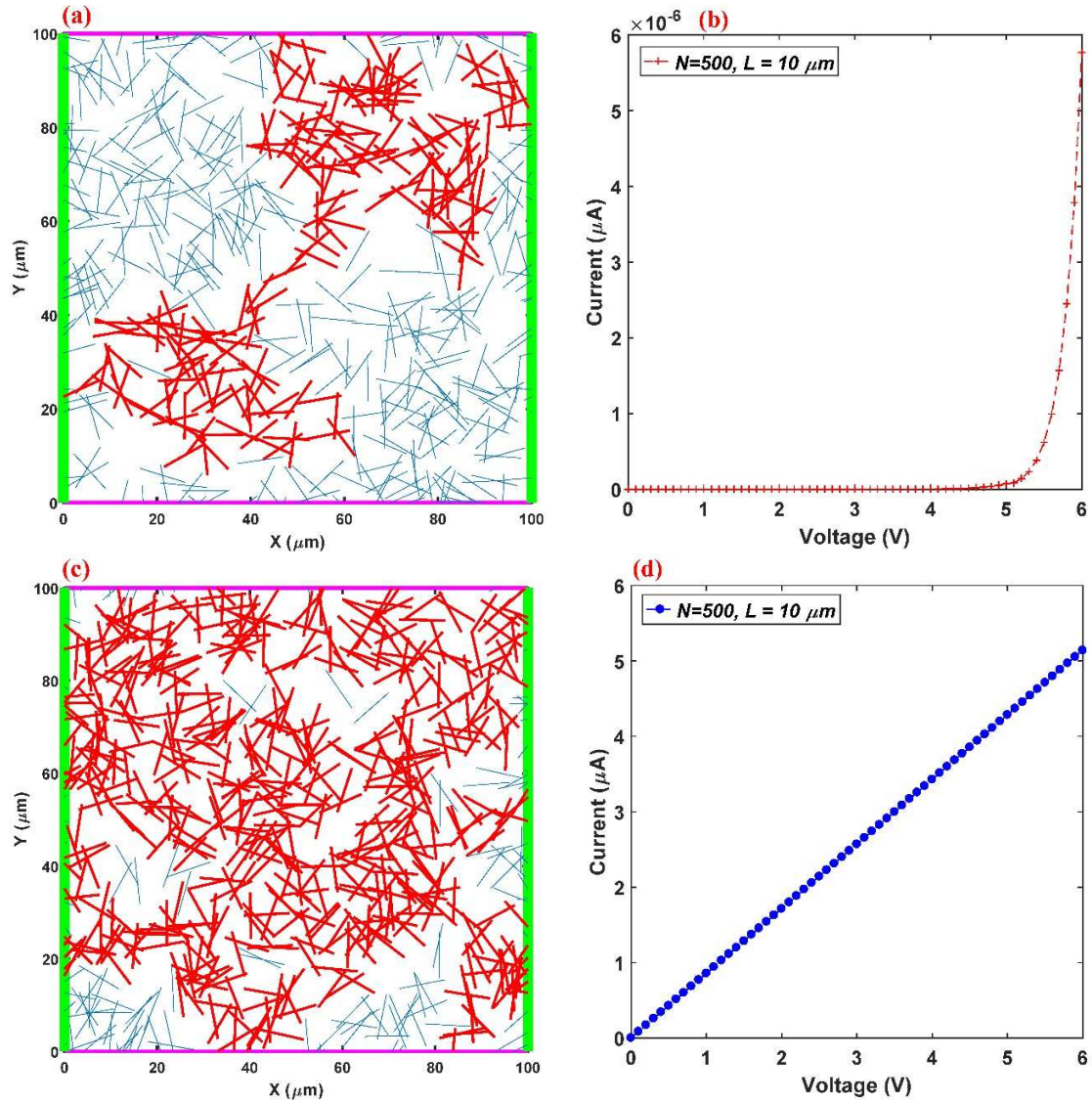


Fig. 8: Representation of CNT distribution with $L_{CNT} = 10 \mu\text{m}$ and: a) $N = 500$, and c) $N = 650$ nanotubes. The corresponding I-V curves of these two microstructures are shown in b) and d), respectively. The RVE size was $100 \times 100 \mu\text{m}^2$. The following parameters were used: $D = 50 \text{ nm}$, $d_{\text{separation}} = 0.47 \text{ nm}$, $g_{CNT} = 10^5 \text{ S/m}$, $K = 3.98$ and $\varphi_0 = 5 \text{ eV}$. In Fig. 8a and c, the percolated clusters are shown in red.

3.3 Model validation

In our previous work [17], the electrical behavior of MWCNT/epoxy nanocomposites was investigated using MWCNT with a diameter of about 50 nm and a length of 20 μm . Different MWCNT weight fractions (0.2, 0.3, and 0.5 wt. %) were used to prepare the nanocomposites with a combination of ultrasonic and shear mixing methods. For direct conductivity (DC) mode, the continuous response of voltage and current were measured for all the samples.

Based on the MWCNT length, the numerical simulations were performed using a unit cell with dimensions of $100 \times 100 \mu\text{m}^2$. The RVE size should be at least four or five times larger than the longest dimension of fillers to achieve reliable results [26]. To compare our numerical and experimental results, the following parameters were chosen in our simulations: $D = 50 \text{ nm}$, $L_{CNT} = 20 \mu\text{m}$, $K = 3.98$, $\varphi_0 = 5 \text{ eV}$ and, $g_{CNT} = 10^5 \text{ S/m}$. The $d_{\text{separation}}$ of 0.47 nm was also used based on the suggestion of Hu et al. [26] for the MWCNT/epoxy system. By fitting the experimental data, CNT densities of $N = 125, 400, \text{ and } 800$ nanotubes were chosen as equivalent concentrations for 0.2, 0.3, and 0.5 wt.% MWCNT in the epoxy nanocomposites, respectively. Both the numerical prediction and experimental results are plotted in Fig. 9 and 10.

Close to the percolation threshold, the bulk I-V response of the system strongly depends on the CNT dispersion quality (i.e., different equivalent length and number of junctions). Depending on the configuration of CNTs, different relations between voltage and current can be obtained. For instance, Fig. 9a presents the I-V curves of four randomly generated configurations of CNTs in the simulation box, per $N= 125$ and $L_{CNT}= 20 \mu\text{m}$. Based on Fig. 4, for $N= 125$ and $L_{CNT}= 20 \mu\text{m}$, the composite is close to the percolation threshold. In this case, as it is obvious in Fig. 9a, the I-V response of the model can be linear, nonlinear, or noisy for the sample with $N= 125$ CNT of $L_{CNT} = 20 \mu\text{m}$. Moreover, different conductive behaviors can be found for different configurations of

CNTs. The respective numerical I-V curve is compared with the 0.2 wt. % MWCNT/epoxy nanocomposite [17] (Fig. 9b). As shown in Fig. 9b, some fluctuations in the experimental results at 0.2 wt.% MWCNT can be seen, which are well captured by the present model using $N= 125$ CNT of $L_{CNT} = 20 \mu\text{m}$. It is worth mentioning that since we are looking for I-V characteristic curve near percolation, the averaging technique over high numbers of run is not a good idea. This is because we have completely different behaviors per different configurations.

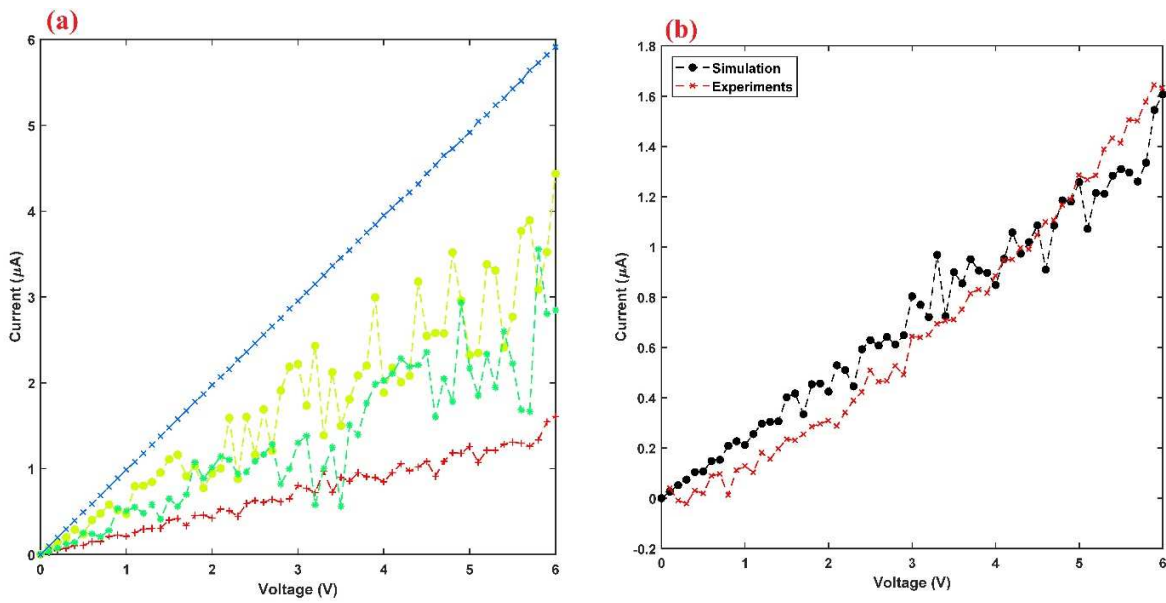


Fig. 9: a) Different behaviors of I-V curve per different configurations of CNTs in the simulation box for $N=125$, and b) Comparison between the numerical and experimental results [17] for 0.2 wt. % MWCNT/epoxy nanocomposites. The simulation constants are assumed to be: $RVE= 100 \times 100 \mu\text{m}^2$, $D = 50 \text{ nm}$, $L_{CNT} = 20 \mu\text{m}$, $d_{\text{separation}} = 0.47 \text{ nm}$, $g_{CNT} = 105 \text{ S/m}$, $K = 3.98$ and $\phi_0 = 5 \text{ eV}$.

The average I-V curve obtained from 20 simulations was compared with the results of the 0.3 wt.% ($N= 400$) and 0.5 wt. % ($N= 800$) MWCNT/epoxy nanocomposite. For these concentrations, the samples are far above percolation, and their respective I-V curves are linear (Fig. 10). In this case, for all the CNT configurations, the predicted I-V curves were linear, and no difference in the conductive behavior of the different microstructures is observed (deviation of less than 0.5% for each level of voltage). This is because far above percolation, the

$\frac{L_{CNT_{percolation}}}{N_{junctions}}$ ratio is almost constant for all the CNT configurations at a fixed CNT content.

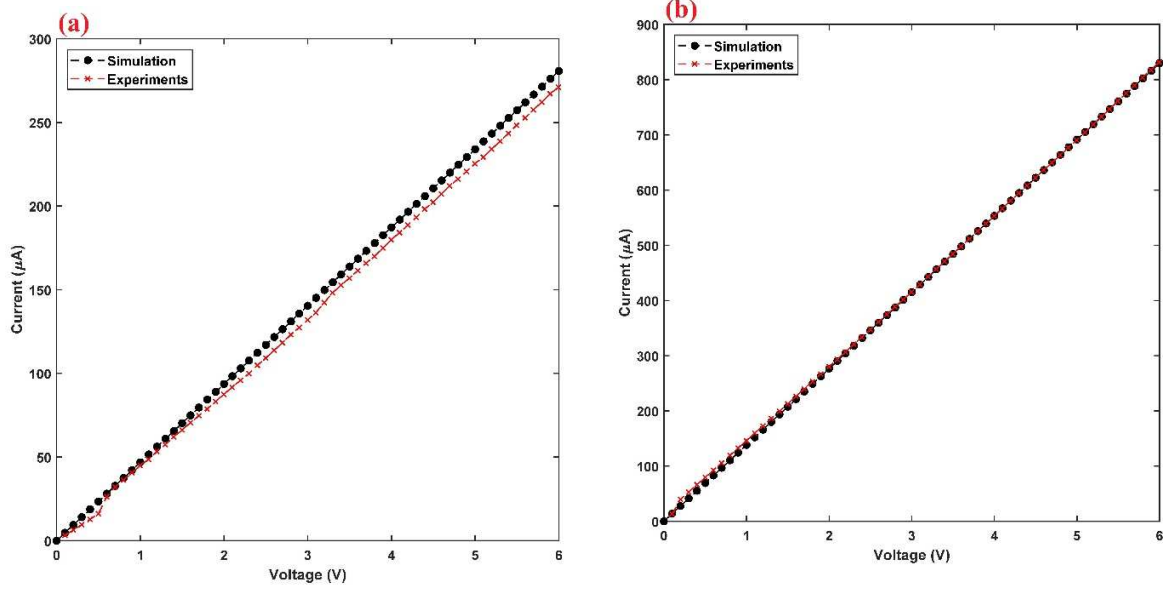


Fig. 10: Comparison between the numerical and experimental results [17] for MWCNT/epoxy nanocomposites with a) $N = 400$ and 0.3 wt.% of MWCNT, and b) $N = 800$ and 0.5 wt.% of MWCNT. In the simulations, the RVE size is $100 \times 100 \mu\text{m}^2$. The other parameters are: $D = 50 \text{ nm}$, $L_{CNT} = 20 \mu\text{m}$, $d_{separation} = 0.47 \text{ nm}$, $g_{CNT} = 105 \text{ S/m}$, $K = 3.98$ and $\phi_0 = 5 \text{ eV}$.

It can be seen in Fig. 9 and Fig. 10 that the numerical predictions are in very good agreement with the experimental results. It should be noted that the present model can evaluate the I-V curve of the CNT/polymer composites without prior knowledge of the percolation threshold.

4. Conclusions

In this study, Simmons' formula was used to consider the tunneling effect on the characteristic I-V curves of carbon nanotube (CNT)/polymer nanocomposites. Based on this approach, a voltage-dependent tunneling resistance was defined at each CNT-CNT junction. A recursive procedure was introduced to evaluate the voltage across each junction, and subsequently, the bulk I-V characteristic curves of the nanocomposites. Our observations showed that the proposed model can successfully capture the nonlinear and noisy behavior of the I-V curve, which is

present for CNT loadings near the percolation threshold, which was also validated by experimental results taken from our previous work. The voltage-dependent nature of the contact resistance was found to be the main reason for this nonlinear and noisy behavior. For more quantitative analysis, a new parameter, namely $\left(\frac{L_{CNT_{percolation}}}{N_{junctions}}\right)$, was proposed to determine the effect of the CNT average length of the linear resistance (i.e., intrinsic nanotubes resistance) per a junction. By increasing the $\frac{L_{CNT_{percolation}}}{N_{junctions}}$ ratio, the I-V curves become less nonlinear and the nanocomposites showed a more conductive behavior. Through Monte Carlo simulations, the I-V curves of CNT/polymer nanocomposites were numerically calculated as a function of CNT diameter, length, and intrinsic conductance, as well as the tunneling gap at the junctions ($d_{separation}$), and the matrix dielectric constant. Based on the results obtained, it was found that $d_{separation}$ and intrinsic CNT conductance (g_{CNT}) are the most important parameters controlling the overall bulk conductivity of CNT/polymer nanocomposites. It is believed that the simulation procedure presented in this work and the way we incorporated the tunneling resistance can provide highly accurate electrical properties predictions for CNT/polymer nanocomposites in 3D mode, especially near the percolation threshold without prior knowledge of its value.

Competing interests

The authors declare that they have no competing interests.

References

[1] Snook GA, Kao P, Best AS. Conducting-polymer-based supercapacitor devices and electrodes. *Journal of Power Sources*. 2011;196(1):1-12.

- [2] Bagotia N, Choudhary V, Sharma DK. A review on the mechanical, electrical and EMI shielding properties of carbon nanotubes and graphene reinforced polycarbonate nanocomposites. *Polymers for Advanced Technologies*. 2018;29(6):1547-67.
- [3] Avilés F, Oliva-Avilés AI, Cen-Puc M. Piezoresistivity, Strain, and Damage Self-Sensing of Polymer Composites Filled with Carbon Nanostructures. *Advanced Engineering Materials*. 2018;20(7):1701159.
- [4] Pandey G, Thostenson ET. Carbon Nanotube-Based Multifunctional Polymer Nanocomposites. *Polymer Reviews*. 2012;52(3):355-416.
- [5] Wu S, Peng S, Wang C. Multifunctional Polymer Nanocomposites Reinforced by Aligned Carbon Nanomaterials. *Polymers*. 2018;10(5):542.
- [6] Yang L, Wang S, Zeng Q, Zhang Z, Peng L-M. Carbon Nanotube Photoelectronic and Photovoltaic Devices and their Applications in Infrared Detection. *Small*. 2013;9(8):1225-36.
- [7] Li C, Thostenson ET, Chou T-W. Dominant role of tunneling resistance in the electrical conductivity of carbon nanotube-based composites. *Applied Physics Letters*. 2007;91(22):223114.
- [8] Bao WS, Meguid SA, Zhu ZH, Weng GJ. Tunneling resistance and its effect on the electrical conductivity of carbon nanotube nanocomposites. *Journal of Applied Physics*. 2012;111(9):093726.
- [9] Lee BM, Loh KJ, Yang Y-S. Carbon nanotube thin film strain sensor models assembled using nano- and micro-scale imaging. *Computational Mechanics*. 2017;60(1):39-49.
- [10] Khromov KY, Knizhnik AA, Potapkin BV, Kenny JM. Multiscale modeling of electrical conductivity of carbon nanotubes based polymer nanocomposites. *Journal of Applied Physics*. 2017;121(22):225102.

- [11] Gbaguidi A, Namilae S, Kim D. Stochastic percolation model for the effect of nanotube agglomeration on the conductivity and piezoresistivity of hybrid nanocomposites. *Computational Materials Science*. 2019;166:9-19.
- [12] Wang G, Wang C, Zhang F, Yu X. Electrical percolation of nanoparticle-polymer composites. *Computational Materials Science*. 2018;150:102-6.
- [13] Gau C, Cheng-Yung K, Ko HS. Electron tunneling in carbon nanotube composites. *Nanotechnology*. 2009;20(39):395705.
- [14] Yu Y, Song G, Sun L. Determinant role of tunneling resistance in electrical conductivity of polymer composites reinforced by well dispersed carbon nanotubes. *Journal of Applied Physics*. 2010;108(8):084319.
- [15] Ounaies Z, Park C, Wise KE, Siochi EJ, Harrison JS. Electrical properties of single wall carbon nanotube reinforced polyimide composites. *Composites Science and Technology*. 2003;63(11):1637-46.
- [16] Hu CH, Liu CH, Chen LZ, Fan SS. Semiconductor behaviors of low loading multiwall carbon nanotube/poly(dimethylsiloxane) composites. *Applied Physics Letters*. 2009;95(10):103103.
- [17] Alizadeh Sahraei A, Ayati M, Baniassadi M, Rodrigue D, Baghani M, Abdi Y. AC and DC electrical behavior of MWCNT/epoxy nanocomposite near percolation threshold: Equivalent circuits and percolation limits. *Journal of Applied Physics*. 2018;123(10):105109.
- [18] Ning H, Zen M, Cheng Y, Go Y, Hisao F, Toshiyuki H. The electrical properties of polymer nanocomposites with carbon nanotube fillers. *Nanotechnology*. 2008;19(21):215701.
- [19] Lee BM, Loh KJ. A 2D percolation-based model for characterizing the piezoresistivity of carbon nanotube-based films. *Journal of Materials Science*. 2015;50(7):2973-83.

- [20] Bo Mi L, Kenneth JL. Carbon nanotube thin film strain sensors: comparison between experimental tests and numerical simulations. *Nanotechnology*. 2017;28(15):155502.
- [21] Hu N, Karube Y, Yan C, Masuda Z, Fukunaga H. Tunneling effect in a polymer/carbon nanotube nanocomposite strain sensor. *Acta Materialia*. 2008;56(13):2929-36.
- [22] Rubaiya R, Peyman S. Effects of inter-tube distance and alignment on tunnelling resistance and strain sensitivity of nanotube/polymer composite films. *Nanotechnology*. 2012;23(5):055703.
- [23] Simmons JG. Generalized Formula for the Electric Tunnel Effect between Similar Electrodes Separated by a Thin Insulating Film. *Journal of Applied Physics*. 1963;34(6):1793-803.
- [24] Simmons JG. Conduction in thin dielectric films. *Journal of Physics D: Applied Physics*. 1971;4(5):613.
- [25] Balberg I, Binenbaum N. Cluster structure and conductivity of three-dimensional continuum systems. *Physical Review A*. 1985;31(2):1222-5.
- [26] Hu N, Karube Y, Arai M, Watanabe T, Yan C, Li Y, et al. Investigation on sensitivity of a polymer/carbon nanotube composite strain sensor. *Carbon*. 2010;48(3):680-7.
- [27] Simmons JG. Electric Tunnel Effect between Dissimilar Electrodes Separated by a Thin Insulating Film. *Journal of Applied Physics*. 1963;34(9):2581-90.
- [28] Hertel T, Walkup RE, Avouris P. Deformation of carbon nanotubes by surface van der Waals forces. *Physical Review B*. 1998;58(20):13870-3.
- [29] Girifalco LA, Hodak M, Lee RS. Carbon nanotubes, buckyballs, ropes, and a universal graphitic potential. *Physical Review B*. 2000;62(19):13104-10.
- [30] Roy S, Akepati AR, Hayes N. Atomistic modeling of fracture properties in nano- particle

reinforced polymers. 27th Annual Technical Conference of the American Society for Composites 2012, Held Jointly with 15th Joint US-Japan Conference on Composite Materials and ASTM-D30 Meeting 2012. p. 574-88.

[31] Darrell HR, Iksoo C. Nanometre diameter fibres of polymer, produced by electrospinning. *Nanotechnology*. 1996;7(3):216.

[32] DeCarlo RA, Lin PM. *Linear Circuit Analysis: Time Domain, Phasor, and Laplace Transform Approaches*: Prentice Hall; 1995.

[33] Shiraishi M, Ata M. Work function of carbon nanotubes. *Carbon*. 2001;39(12):1913-7.

[34] Zeng X, Xu X, Shenai PM, Kovalev E, Baudot C, Mathews N, et al. Characteristics of the Electrical Percolation in Carbon Nanotubes/Polymer Nanocomposites. *The Journal of Physical Chemistry C*. 2011;115(44):21685-90.

[35] deHeer WA, Bacsá WS, Châtelain A, Gerfin T, Humphrey-Baker R, Forro L, et al. Aligned Carbon Nanotube Films: Production and Optical and Electronic Properties. *Science*. 1995;268(5212):845-7.

[36] Rei H, Shinya Y, Takashi I, Mitsuhiro K, Norihiro Y, Winadda W, et al. Electronic Transport in Multiwalled Carbon Nanotubes Contacted with Patterned Electrodes. *Japanese Journal of Applied Physics*. 2004;43(8B):L1081.

